Theory of unconventional quantum Hall effect in strained graphene

Bitan Roy[1], Zi-Xiang Hu[2,3], Kun Yang[1]
[1] *National High Magnetic Field Laboratory, Florida State University, FL 32306, USA*
[2] *Department of Physics, Chongqing University, Chongqing 400044, China*
[3] *Department of Electrical Engineering, Princeton University, Princeton, New Jersey 08544, USA*
(Dated: November 21, 2012)

We show through both theoretical arguments and numerical calculations that graphene discerns an unconventional sequence of quantized Hall conductivity, when subject to both magnetic fields (B) and strain. The latter produces time-reversal symmetric pseudo/axial magnetic fields (b). The single electron spectrum is composed of two inter-penetrating sets of Landau levels (LLs), located at $\pm\sqrt{2n|b \pm B|}$, $n = 0, 1, 2, \cdots$. For $b > B$, these two sets of LLs have opposite *chiralities*, resulting in *oscillating* Hall conductivity between 0 and $\mp 2e^2/h$ in electron and hole doped system, respectively, as the chemical potential deviates from the neutrality point, but remains in its vicinity. The electron-electron interactions stabilizes various correlated ground states, e.g., spin-polarized, quantum spin-Hall insulators at and near the neutrality point, and possibly anomalous Hall insulating phase at incommensurate filling $\sim B$. Such broken symmetry ground states have similarities as well as significant differences from there counterparts in the absence of strain. For realistic strength of magnetic fields and interactions, we present scaling of interaction induced gap for various Hall states within the zeroth Landau level.

PACS numbers: 71.10.Pm, 71.10.Li, 05.30.Fk, 74.20.Rp

Successful fabrication of two-dimensional electron gas (2DEG), e.g., Galium-Arsenide (GaAs) heterostructure, provided unique opportunity to observe a peculiar novel aspect of low-dimensional electronic systems, quantization of Hall conductivity (σ_{xy}). At weaker magnetic fields ($\sim$ 1 T), even the samples with lower mobilities, discern quantized plateaus of σ_{xy} at various integer values of e^2/h. This phenomena is referred to as *integer quantum Hall effect* (IQHE) [1]. Rather more striking observation is the plateaus of that quantity at various, for example 1/3, fractions of e^2/h, in improved samples, however at stronger fields ($\sim$ 10 T) [2]. Whereas the IQHE arises from free motion of fermions in magnetic field [3], its fractional version necessarily requires strong electron-electron interactions to develop mobility gap within a partially filled Landau level [4].

Integer quantization of σ_{xy} appears when the chemical potential (μ) lies within a mobility gap, filled by localized states, separated by two extended conducting edge modes, carrying the quantized Hall current [5]. As the magnetic field is reduced, more and more extended states get occupied and the total Hall current, which is the *algebraic* sum of the Hall current carried by each of them, encounters quantized increment, due to the identical *chirality* of all the extended edge states, placed at well separated energies [6].

Besides the GaAs heterostructure, the new generation two-dimensional electronic system, *graphene*, discerns a sequence of Hall plateaus at fillings $\nu = \pm 4(n + \frac{1}{2})$, subject to relatively low fields [7], while additional plateaus, for example at $\nu = 0, \pm 1, \pm 4$, show up as the field is enhanced [8, 9]. Otherwise, all the LLs support the current carrying states with identical chirality, as in GaAs [10]. However, due to its mechanical flexibility under strain and the underlying hexagonal crystallographic arrangement, graphene may experience yet another magnetic field, which may emerge from its bulging [11]. Such strain induced pseudo/axial magnetic field preserves the time reversal symmetry (TRS), and points in opposite directions at two inequivalent Dirac points, suitably chosen here at $\vec{K} = (1, 1/\sqrt{3})(2\pi/a\sqrt{3})$ and $-\vec{K}$ [12]. Therefore, subject to strain as well as an external magnetic field, one can expose the gapless Dirac quasi-particles, near two Dirac points with different effective fields, $|B \pm b|$, possibly pointing in *opposite* directions, respectively. Hence, an interplay of these two gauge fields, concomitantly an unconventional spectrum of the Hall conductivity can be realized in graphene.

It is perhaps worth considering the Hall response of this system when $B > b(\neq 0)$ first, though such condition may not be achieved in laboratory at this moment [13]. The spectrum of non-interacting Dirac quasiparticles is comprised of two inter-penetrating sets of LLs at well separated energies $\pm\sqrt{2n(B \pm b)}$ with degeneracies $(B \pm b)/2\pi$ per unit area. A previous work predicts that quantized Hall conductivity then may appear at all the integer values of e^2/h, however they occur at incommensurate fillings, due to distinct degeneracies of two sets of LLs [14]. The monotonic variation of the Hall conductivity arises from the fact that all the LLs experience the orbital effect of the effective magnetic fields in the same direction, yielding the current carrying extended states with identical chirality. Hence upon increasing electron or hole doping, as the chemical potential sweeps through various LLs, the total Hall current adds up, leading to the announced spectrum of σ_{xy}.

Rather more interesting situation arises when $b > B$. For $B = 0$, the pseudo Dirac LLs, spaced at $\pm\sqrt{2nb}$ [15–18], and near two valleys have opposite chirality, henceforth the TRS is preserved. As long as $b > B > 0$, two inequivalent sets of LLs, now located at $\sqrt{2n(b \pm B)}$, with respective degeneracies $(b \pm B)/2\pi$, per unit area, con-

tinue to enjoy opposite chirality (see left column of Fig. 1). Consequently, as the chemical potential starts to deviate from the charge neutrality point (CNP), the Hall conductivity is restricted within $\pm 2e^2/h$ (when more LLs localized near one valley is filled) and 0 (equal number of LLs localized near two Dirac points are populated). The $\pm$ sign corresponds to hole and electron doped systems, respectively, and note it is *opposite* to what one has in the absence of the strain-induced field, b.

Even though the Hall conductivity stays bounded, as the chemical potential is enhanced, more and more current carrying edge states get filled. Therefore, in a two terminal conductance measurement, its longitudinal component G_{xx} is expected to increase monotonically. Every time the Hall conductivity suffers a quantized change, the two terminal longitudinal conductance G_{xx} increases by $2e^2/h$ (see right column of Fig. 1)[20]. However, the oscillatory sequence of σ_{xy} is strictly true, in the vicinity of the CNP. The spacing of the Dirac LL decreases with the LL index and the effective magnetic field experienced by these sets of LLs are different. Hence, far away from the CNP, LL crossing is unavoidable, and the above mentioned spectrum of Hall conductivity may cease. One can then in principle observe quantized plateaus of σ_{xy} at higher integer values $\geq 3e^2/h$. When $B \ll b$, the LL crossing occurs at large LL index (n). In that limit, assuming that the chemical potential is not too far from the Dirac points, one can safely neglect the LL crossing. Upon incorporating the Zeeman splitting, $\Delta_z \sim B$ (T) K, additional Hall plateaus appears at $\sigma_{xy} = \pm e^2/h$, in between 0 and $\pm 2e^2/h$.

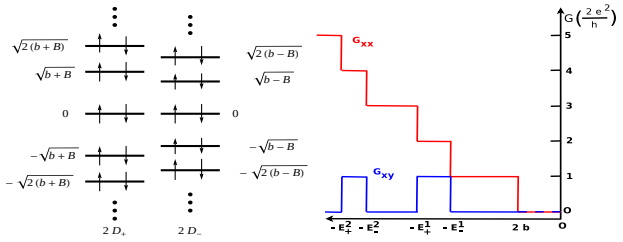

FIG. 1: (Color online) Left: Spin degenerate interpenetrating LLs of $H_D[A,a]$. Here we have shown the LLs for $n = 0, \pm 1, \pm 2$ only. Two LLs have the degeneracies $2D_\pm = (b \pm B)$ per unit area. Right: Schematic variation of Hall conductances G_{xy} (blue), and two terminal conductances G_{xx} (red) as the chemical potential is tuned in a hole doped graphene. Here, $E_\sigma^n = \sqrt{2n(b+\sigma B)}$, with $\sigma = \pm$. In electron doped system, G_{xx} remains the same, while G_{xy} changes its sign.

To compute the LL spectrum, we here construct an 8-component Dirac spinor $\Psi = (\Psi_\uparrow, \Psi_\downarrow)^\top$, where $\Psi_\sigma^\top = [u_\sigma^\dagger(\vec{K}+\vec{q}), v_\sigma^\dagger(\vec{K}+\vec{q}), u_\sigma^\dagger(-\vec{K}+\vec{q}), v_\sigma^\dagger(-\vec{K}+\vec{q})]$, with $\sigma = \uparrow, \downarrow$ as electrons spin projection along the $z-$direction. The orbital effects of the real and pseudo magnetic fields can be captured by the Hamiltonian [14–16]

$$H_D[A,a] = I_2 \otimes i\gamma_0\gamma_i\left(\hat{q}_i - A_i - i\gamma_3\gamma_5 a_i\right). \qquad (1)$$

The magnetic fields are related to the vector potentials as $B(b) = \epsilon_{3ij}\partial_i A(a)_j$. The gamma matrices are $\gamma_0 = I_2 \otimes \sigma_3$, $\gamma_1 = \sigma_3 \otimes \sigma_2$, $\gamma_2 = I_2 \otimes \sigma_1$, $\gamma_3 = \sigma_1 \otimes \sigma_2$, $\gamma_5 = \sigma_2 \otimes \sigma_2$ [19]. The spectrum of $H_D[A,a]$ is comprised of two sets of *interpenetrating* LLs at energies $\pm\sqrt{2n(b+B)}$ and $\pm\sqrt{2n(b-B)}$, with respective degeneracies $\Omega(b \pm B)/2\pi$, shown in Fig. 1 [21]. Here $n = 0, 1, 2, \cdots$ and Ω is the area of the strained graphene sample. With $b > B$ states within the zeroth LL (ZLL) are localized on only one sub-lattice, say A for example, while they reside on complimentary sub-lattices near two Dirac points if $B > b$ [14]. Otherwise, there are $2(b \pm B)$ states per unit area respectively near the Dirac points. The two-fold degeneracy of each LLs is due to fermion spin. The valley degeneracy for all the LLs at finite energies are removed, as they are exposed to different *effective* magnetic fields. However, at precise zero energy LLs can be found near two Dirac points, guaranteed by an 'index theorem'. [23, 24]

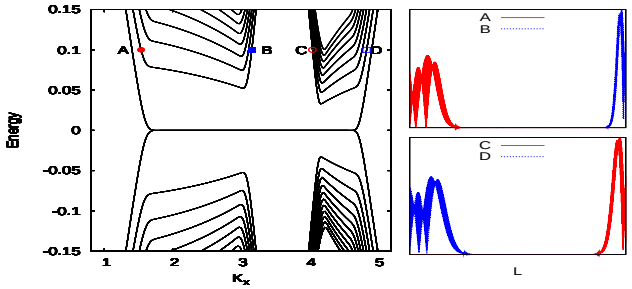

FIG. 2: (Color online) The energy spectrum (left) and wavefunctions (WFs) (right) for a strained graphene in magnetic field when $B < b$. WFs localized on one edge, live on opposite side at two valleys, explicitly, A(B) and D (C) are localized on left (right) edge, therefore carrying opposite chirality.

Let us firsts register the Hall response of the non-interacting system. At $\mu = 0$, the ZLL is half-filled, containing total $4\Omega b$ states. A particle-hole symmetry, generated by $I_2 \otimes \gamma_0$ for example, anti-commute with $H_D[A,a]$; of the spectrum then guarantees exact *zero* Hall conductivity, $\sigma_{xy} = 0$. Upon doping, when the chemical potential is placed between the ZLL and $\sqrt{b-B}$, σ_{xy} remains at zero. It can be seen easily after subscribing the Středa formula [25] for the Hall conductivity $\sigma_{xy} = \left(\frac{\partial N}{\partial B}\right)_\mu$, in the natural units $e = c = 1$. N is the electronic density in the bulk below the chemical potential. Derivative with respect to B is taken at fixed μ, measured from the half-filled band. In order to place the chemical potential such that $0 < \mu < \sqrt{b-B}$, one needs to fill $N = 2\Omega b$ (independent of B) states from the CNP, yielding a *zero* Hall conductivity. On the other hand, if $\sqrt{b-B} < \mu < \sqrt{b+B}$, $\delta N = -2\delta B$ and hence $\sigma_{xy} = -2$. The factor 2 counts the spin degeneracy of the LL. Upon further doping when $\sqrt{b+B} < \mu < \sqrt{2(b-B)}$, the Hall conductivity comes back to *zero*. Hence, with odd (even) number (modulo 2 due to spin) of LLs below the chemical potential, one gets $\sigma_{xy} = -2(0)$, as long as

there is no LL crossing. The underlying reason for such oscillatory nature of the Hall conductivity is the following: two sets of LLs near $\pm K$ experience total effective magnetic fields $(b \pm B) > 0$, which point in opposite *directions* and hence the current carrying extended states of these two LLs have opposite *chirality*. When odd number (modulo 2) of LLs above the CNP are filled, $\sigma_{xy} = -2$, since there is imbalance in the occupation of the LLs near two Dirac points. With an even number (modulo 2) of filled LL $\sigma_{xy} = 0$, as the Hall currents from the LLs near $+\vec{K}$ and $-\vec{K}$ exactly cancels each other. With hole dopping, the Hall conductivity oscillates between 0 and $+2\, e^2/h$.

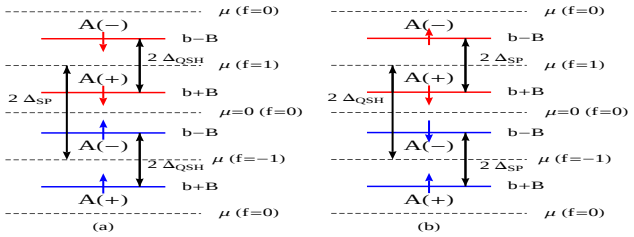

FIG. 3: (Color online) Two possible interaction driven splitting of the zeroth Landau level and spectrum of the Hall conductivity, $\sigma_{xy} = fe^2/h$, at various chemical doping. $\pm$ corresponds to the ZLL states localized near the valley at $\pm\vec{K}$.

The chiral nature of the edge modes in the presence of strain and magnetic field can also be seen in a finite honeycomb lattice, with zigzag edge. The orbital effect of the real magnetic field can be captured by attaching a Peierls phase, $t_{ij} \to t_{ij} \exp\left(2\pi i \frac{e}{hc} \int_i^j \vec{A} \cdot d\vec{l}\right)$ to the nearest-neighbor (NN) hopping amplitudes. The strain induced axial gauge fields can be incorporated in the system by local modulation of the NN hopping amplitudes. We here modify the hopping only along one of the three bonds, oriented orthogonal to the zigzag edge [21, 22]. With such simple deformation, even though one ends up with slightly inhomogeneous Fermi velocities and thus LL engergies, it is still sufficient to capture the peculiarities of the edge modes arising from the preserved TRS. One can see from Fig. 2 that the chiralities of two states localized near one zigzag edge of the system are opposite, if $b > B$, same when $B = 0$, but $b \neq 0$.[21] However, the LLs near two Dirac points appears at different energies. Therefore, as one changes the chemical potential the Hall conductivity keeps oscillating between $\pm e^2/h$ and 0 (since we consider spinless fermion here). If on the other hand, the real magnetic gets stronger, i.e., $B > b$, the edge modes near two Dirac points share identical chiralities.[21] Therefore, when the chemical potential varies, σ_{xy} changes monotonically.[14] An interesting possibility is $B = b$, keeping only one of the Dirac points exposed to finite magnetic field, yielding plateaus of σ_{xy} at $\nu = 2(n + \frac{1}{2})$. The other one remains semi-metallic, giving finite σ_{xy} and σ_{xx} simultaneously.[21, 26]

The Zeeman splitting (Δ_z) lifts the spin degeneracy from all the LLs, including the ZLL, $\sqrt{n(b \pm B)} \to \sqrt{n(b \pm B)} \pm \Delta_z$. As the Zeeman gap scales as $\Delta_z \sim B$ K ($\ll \sum_{\sigma=\pm} \sigma \sqrt{n(b + \sigma B)}$), if B is measured in Tesla, it does not cause LL crossing near the CNP. Otherwise, the Hall conductivity remains pinned to *zero*, when $\mu = 0$ due to the particle-hole symmetry, generated by $\sigma_1 \otimes \gamma_0$, for example. It remains so even when the chemical potential lies in between the Zeeman shifted ZLL at Δ_z and $\sqrt{b - B} - \Delta_z$, because $\delta N = 2b\Omega$ (independent of B). Otherwise for $\sqrt{b + \sigma B} + \sigma\Delta_z < \mu < \sqrt{b + \sigma B} - \sigma\Delta_z$, $\sigma_{xy} = -\left(\frac{3+\sigma}{2}\right) e^2/h$, where $\sigma = \pm 1$. Therefore, the Zeeman splitting introduces additional Hall plateau at $\mp e^2/h$, in electron and hole doped systems, respectively.

Due to the peculiar entanglement of the ZLL with the sub-lattice degrees of freedom (all the states are localized on one sub-lattice), a strain induced charge density wave order (not spontaneously generated) always persists within the ZLL. Nevertheless, this configuration is a natural ground state for the residual NN Coulomb repulsion. Since two valleys are populated by distinct number of states, a 'valley polarized' quantum anomalous Hall state cannot develop at CNP. It may however be realized at incommensurate filling, $\nu \propto B$ about the neutrality point. Upon occupying two valleys with opposite spin projections, a spin Hall state, corresponds to circulating currents among the sites of same sublattices of honeycomb lattice, can be realized. It also carries a finite *ferromagnetic* moment, $\propto B$ (difference of LL degeneracies). Since the ZLL is localized on one sub-lattice, the ferromagnet (FM) order is tied with an anti-ferromagnet (AF) order. The spin Hall order parameter reads as $\Delta_{QSH} = \langle \Psi_\sigma^\dagger \vec{\sigma} \otimes i\gamma_1\gamma_2 \Psi_\sigma \rangle$.[27, 28] In the absence of the gauge fields, though it requires finite strength of the second neighbor interaction (V_2) to trigger such ordering [29], even an infinitesimal V_2 can develop a finite spin Hall order, when the kinetic energy of the Dirac quasi-particles is quenched by the axial fields [15–18] and to the leading order $\Delta_{QSH} \propto V_2$ [30]. The spin polarized (SP) state carries finite FM (Δ_{FM}) and AF ($\Delta_{AF} = \langle \Psi_\sigma^\dagger \vec{\sigma} \otimes \gamma_0 \Psi_\sigma \rangle$) orders simultaneously [16]. Though the Zeeman effect yields $\Delta_{FM} \neq 0$, the onsite-Hubbard interaction (U), which is possibly the strongest interaction in graphene [31], prefers an AF ordering, in the vicinity of the CNP. A similar spin polarized state can also be realized even when $B = 0$ [17]. However, in Ref. [17] SP state was identified as pure ferromagnet, which appears to be limited in light of above discussion. The AF order parameter anti-commutes with $H_D[A, a]$. Hence, apart from splitting the ZLL, it optimally lowers the energy of the filled Dirac sea, by pushing all the LLs at finite energies further down, $\pm\sqrt{2n(b \pm B)} \to \pm\sqrt{2n(b \pm B) + \Delta_{AF}^2}$. The spin-polarized gap within the ZLL is $\Delta_{SP} = \Delta_{AF} + \Delta_{FM} \sim U$.

For small Zeeman coupling one can write the ground state energy per unit area at half filling in the presence

of AF ($\vec{N}$) and spin Hall ($\vec{C}$) orders as

$$E[\vec{N},\vec{C}] = \frac{\vec{N}^2}{4g_a} + \frac{\vec{C}^2}{4g_c} + E_0[\vec{N},\vec{C}], \quad (2)$$

where $g_{a(c)} \sim U(V_2)$. $E_0[\vec{N},\vec{C}]$ is the ground state energy per unit area of the effective single particle Hamiltonian

$$H_{HF} = H_D[A,a] - \left(\vec{N}\cdot\vec{\sigma}\right)\otimes\gamma_0 - \left(\vec{C}\cdot\vec{\sigma}\right)\otimes i\gamma_1\gamma_2. \quad (3)$$

With small Zeeman coupling spin-anisotropy can be neglected and we set $\vec{N}(\vec{C}) = (N(C),0,0)$, for simplicity. Minimization of $E[N,C]$, with respect to N and C, yields *two* coupled gap equations, which for $N > C$ reads as

$$\frac{\pi^{3/2}}{2g_i} = \frac{\xi_i}{X_i} + \sum_{n\geq 1,\alpha=\pm}^{i\neq j}\left(\frac{b+\alpha B}{2e_{n,\alpha}} + \frac{X_j}{X_i}\alpha\frac{b+\alpha B}{2e_{n,\alpha}}\right) \quad (4)$$

for $i,j = 1,2$, where $g = (g_a, g_c), X = (N,C), \xi = (b,B)$ and $e_{n,\alpha} = [2n(b+\alpha B) + (N+\alpha C)^2]^{1/2}$. The first term in the gap equations are ultra-violet divergent and independent of X_i. However, cut-off independence of the gap, demands $g_a \equiv g_c$ for both AF and spin Hall order to be simultaneously finite. Since, in graphene, $U > V_2$, possibly a spin polarized state ($N \equiv \Delta_{AF} \neq 0, C \equiv \Delta_{QSH} = 0$) is formed at the CNP. Even though, with $b > B$, there exists a series of $\sigma_{xy} = 0$ plateau, only the one near $\mu = 0$ bears an AF order, while the rest arises from lack of 'valley reflection symmetry'. Placing the chemical potential close to the first excited state at $\pm\Delta_{SP}$, a spin Hall order develops additional incompressible Hall state, leading to $\sigma_{xy} = \pm e^2/h$ (see left column of Fig. 3). If on the other hand, $V_2 > U$, yielding $C > N$, the splitting of the ZLL gets reversed (Fig. 3, right column).

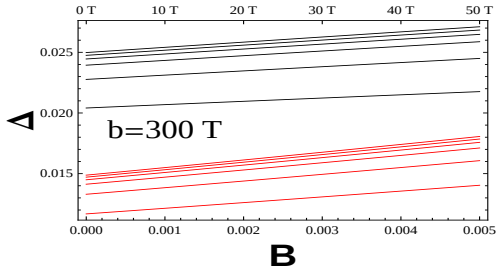

FIG. 4: (Color online) Dimensionless activation gap (Δ/Λ) for $\sigma_{xy} = 0, \pm e^2/h$ (black, red) Hall states when $b = 300$ T and $0\text{ T} < B < 50$ T, for $\delta = 0, 0.03, 0.07, 0.14, 0.3, 0.7$ (from top to bottom), assuming $\Lambda \sim 1/2.5\mathring{A}$, the ultra-violet cutoff over which the dispersion is approximately linear. g_c is the zero field criticality. Lower x-axis denotes B/Λ^2 (dimensionless).

Minimizing the ground state energy, one can find the gap equation for $\sigma_{xy} = 0$ plateau near the CNP. For fixed axial magnetic field ($b = 300T$), the interaction induced gap at the neutrality point increases linearly with the real magnetic field ($0\text{ T} < B < 50$ T) (See Fig. 4), since with increasing B LLs at lower energies ($-e_{n,+}$) is pushed further down and also their degeneracies ($\sim b + B$) increases. Otherwise the gap is insensitive to exact nature of the order parameter. Scaling of the activation gap for $\sigma_{xy} = \pm e^2/h$ state within the ZLL is qualitatively same as (however smaller than) that for $\sigma_{xy} = 0$. Such hierarchy comes solely from the ZLL, as exactly half of the ZLL contributes to the gap for $\sigma_{xy} = 0$ state, while a fewer states within the ZLL contribute to the $\sigma_{xy} = \pm 1$ state. [21]. Otherwise, activation gap for both the Hall state, scales sub-linearly with the strength of the interaction, $\delta = (g\Lambda)^{-1} - (g_*\Lambda)^{-1}$, where g_* is zero field criticality for insulation. If either of the magnetic fields becomes *inhomogeneous*, the LLs at finite energies get distorted, however the ZLL stays unaffected. Therefore, interaction induced gap generation take place even when the field is non-uniform, whereas the gaps then closely follow profile of the magnetic fields.[24] With weak inhomogeneous fields, the quantization of σ_{xy} is expected to survive.

In the absence of the axial field or even when $B > b$, the states within the ZLL, localized near two valleys live on complimentary sub-lattices [14, 32]. Therefore, a conventional AF order develops by filling up states on two sublattices with opposite spin projections, if the onsite repulsion is strong enough. However, the staggered spin moments on two sub-lattices are of different magnitudes. Therefore, one may argue such a correlated phase as *ferrimagnetic* as well [14]. On the other hand, when $b > B$, the AF state is formed by filling states in ZLL, with a particular spin projection, living on one sub-lattice.

In experiment [11], the axial field is localized only in certain region of the sample, however it is *uniform*. Particles circling the axial field inducing bumps can pick up an axial Aharonov-Bohm phase (ABP), only if it travel through the strained region. Otherwise, it is identical for the trajectories in opposite directions, whereas the ABP due to the real magnetic field are of opposite sign for the trajectories in opposite directions [33]. Consequently, the trajectories with opposite circulation, acquires different effective ABP, namely, sum and difference of it due to two fields. Therefore, in Hall conductivity measurement, the terminals need to be attached to the regions with at least finite strain, since the axial gauge potential is proportional to strain, though b can be zero. In *molecular graphene*[34], and recently fabricated strained graphene on Ru substrate [35], the axial field can possibly be realized in the entire sample, thereby may easily discern the peculiar Hall conductivity, we propose here.

Author B.R. acknowledges the support by National Science Foundation Cooperative Agreement No. DMR-0654118, the State of Florida, and the U.S. Department of Energy. Z. X. H. is supported by NSFC No. 11274403 and DOE grant No. de-sc0002140. K. Y. is supported by NSF grant No. DMR-1004545. B. R. is grateful to Igor F. Herbut for many useful discussions. B.R. thanks École de Physique, Les Houches for hospitality during the summer school "Strongly interacting quantum systems out of equilibrium", where part of the manuscript was prepared.

[1] K. von Klitzing, G. Dorda, M. Pepper, Phys. Rev. Lett. **45**, 494 (1980).
[2] D.C. Tsui, H.L. Stormer, A.C. Gossard, Phys. Rev. Lett. **48**, 1559 (1982).
[3] *Quantum Hall Effect*, edited by R. E. Prange and S. M. Girvin (Springer-Verlag, New York, 1989).
[4] R. B. Laughlin, Phys. Rev. Lett. **50**, 1395 (1983).
[5] B. I. Halperin, Phys. Rev. B **25**, 2185 (1982).
[6] R. B. Laughlin, Phys. Rev. B **23**, 5632 (1981).
[7] K.S. Novoselov, A. K. Geim, S. V. Morozov, D. Jiang, and M. I. Katsnelson, Nature (London), **438**, 197 (2005); Y. Zhang, Y.-W. Tan, H. L. Stormer, P. Kim, Nature (London), **438**, 201 (2005).
[8] Y. Zhang, Z. Jiang, J. P.Small, M. S. Purewal, Y.-W. Tan, M. Faziollahi, J. D. Chudow, J. A. Jaszczak, H. L. Stormer, P. Kim, Phys. Rev. Lett. **96**, 136806 (2006).
[9] For a recent review, see, *e.g.*, Y. Barlas, Kun Yang, and A. H. MacDonald, *Nanotechnology* **23**, 052001 (2012).
[10] With only B, particle and hole LLs have opposite chirality, hence $\nu\epsilon \pm \mathcal{Z}$.
[11] N. Levy, S. A. Burke, K. L. Meaker, M. Panlasigui, A. Zettl, F. Guinea, A. H. Castro Neto, and M. F. Crommie, Science, **329**, 544 (2010).
[12] G. W. Semenoff, Phys. Rev. Lett. **53**, 2449 (1984).
[13] Typically $b \sim 300$ T [11, 35], but $B_{max} \sim 45$ T.
[14] B. Roy, Phys. Rev. B **84**, 035458 (2011); *ibid* **85**, 165453 (2012).
[15] I. F. Herbut, Phys. Rev. B **78**, 205433 (2008).
[16] B. Roy and I. F. Herbut, unpublished. See also, B. Roy, Ph.D. thesis, Simon Fraser University, 2011.
[17] P. Ghaemi, J. Cayssol, D. N. Sheng, A. Vishwanath, Phys. Rev. Lett, **108**, 266801 (2012).
[18] D. A. Abanin, D. A. Pesin, Phys. Rev. Lett. **109**, 066802 (2012).
[19] I. F. Herbut, et. al., Phys. Rev. B **79**, 085116 (2009).
[20] This is strictly true only in the absence of back-scattering between edge modes with opposite chiralities, propagating along the *same* edge. Though, it may be weak as long as it comes from smooth scattering potentials, since such modes come from different Dirac points.
[21] See supplementary material.
[22] Y. Chang, T. Albash, and S. Hass, Phys. Rev. B **86**, 125402 (2012).
[23] Y. Aharonov and C. Casher, Phys. Rev. A **19**, 2461 (1979).
[24] B. Roy and I. F. Herbut, Phys. Rev. B **83**, 195422 (2011).
[25] P. Středa, J. Phys. C **15**, L717 (1982).
[26] T. Low and F. Guinea, Nano Lett. **10**, 3551 (2010).
[27] F. D. M. Haldane, Phys. Rev. Lett. **61**, 2015 (1988).
[28] B. Roy and I. F. Herbut, Phys. Rev. B **82**, 035429 (2010).
[29] S. Raghu, X.-L. Qi, C. Honerkamp, S.-C. Zhang, Phys. Rev. Lett. **100**, 156401 (2008).
[30] I. F. Herbut, B. Roy, Phys. Rev. B **77**, 245438 (2008).
[31] T. O. Wohling, E. Şaşıoğlu, C. Friedrich, A. I. Lichtenstein, M. I. Katsnelson, S. Blügel, Phys. Rev. Lett. **106**, 236805 (2011).
[32] I. F. Herbut, Phys. Rev. B **75**, 165411 (2007); J. Jung and A. H. MacDonald, Phys. Rev. B **80**, 235417 (2009).
[33] F. de Juan, A. Cortijo, M. A. H. Vozmediano, A. cano, Nat. Phys. **7**, 810 (2011); Y. Aharonov, D. Bohm, Phys. Rev. **115**, 485 (1959).
[34] K. K. Gomes, W. Mar, W. Ko, F. Guinea, H. Manoharan, Nature **483**, 306 (2012).
[35] J. Lu, A. H. Castro Neto, K. P. Loh, Nature Comm. **3**, 823 (2012).

Supplementary material for "Theory of unconventional quantum Hall effect in strained graphene"

I. DIAGONALIZATION OF DIRAC HAMILTONIAN IN REAL AND AXIAL MAGNETIC FIELDS

We here present one possible prescription to diagonalize the Dirac Hamiltonian in the presence of real and strain induced pseudo/axial magnetic fields. Recall, the low energy Hamiltonian in graphene, subject to strain and magnetic field reads as [1]

$$H_D\left[A,a\right] = I_2 \otimes i\gamma_0\gamma_i\left(\hat{q}_i - A_i - i\gamma_3\gamma_5 a_i\right). \qquad (5)$$

The axial vector potential (a_i) is a member of general $SU(2)$ time reversal symmetric gauge potential

$$a_i = \gamma_3 a_i^3 + \gamma_5 a_i^5 + i\gamma_3\gamma_5 a_i^{35}. \qquad (6)$$

However, the first two terms break the translational symmetry, generated by $I_{tr} = I_2 \otimes i\gamma_3\gamma_5$. If the deformation of the graphene flake is smooth enough one can safely neglect their contributions and only keep the a_i^{35} component. Upon setting $a_i^3 = a_i^5 = 0$, we set $a_i^{35} \equiv a_i$, for notational simplicity. Thereafter, the Dirac Hamiltonian is devoid of any valley mixing. One can then exchange the second and the third 2×2 blocks of $H_D[A,a]$ and cast it in a block diagonal form, say $H_+ \oplus H_-$, where

$$H_\pm = \pm I_2 \otimes \sigma_1(\hat{q}_1 \mp a_1 - A_1) + I_2 \otimes \sigma_2(\hat{q}_2 \mp a_2 - A_2). \quad (7)$$

$H_\pm$ capture the effect of both the gauge potentials on the Dirac fermions in the vicinity of $\pm\vec{K}$ points, respectively. However, both $H_\pm$ are unitarily equivalent to the celebrated Dirac Hamiltonian, $H_D = i\gamma_0\gamma_i(\hat{q}_i - A_i^{ef})$, subject

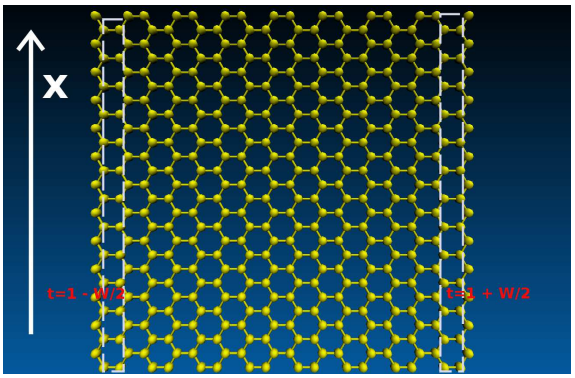

FIG. 5: (Color online) Graphene with zigzag edges. The edge (along x direction) is effectively infinite and the width in y direction is finite. In the strained case, we suppose the hopping terms along y direction has a gradient which ranges from $t = 1 - W/2$ to $t = 1 + W/2$ from one side to the other.

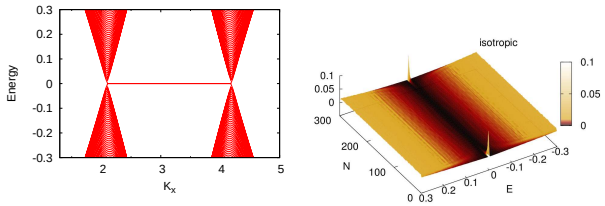

FIG. 6: (Color online) The low energy spectrum (left) and the local density of states (LDOS) (right) for isotropic graphene sheet which has infinite length in x direction and finite width of $N = 300$ unit cells in y direction. The zero energy edge states exist between two Dirac points and contribute peaks in the LDOS.

to effective magnetic fields, $b \pm B$ respectively. Explicitly, $H_+ = U_1^\dagger H_D U_1$, with $U_1 = I_2 \oplus i\sigma_2$ and $A_i^{ef} = a_i + A_i$, while $H_- = U_2^\dagger H U_2$, with $U_2 = i\sigma_2 \oplus I_2$ and $A_i^{ef} = a_i - A_i$ [1, 2]. After expressing the original Hamiltonian $H_D[A, a]$ as direct sum of two inequivalent copies of the standard Dirac Hamiltonian subject to different effective magnetic fields, one can immediately diagonalize it, yielding the announced spectrum of inter-penetrating sets of Landau levels (LLs) [3].

II. NUMERICAL DIAGONALIZATION OF NON-INTERACTING HAMILTONIAN IN STRAINED FINITE SIZE GRAPHENE, SUBJECT TO MAGNETIC FIELDS

We consider a single layer graphene with infinite length in x direction and finite width of N unit cells in y direction as shown in Fig. 5. The tight-binding Hamiltonian for spinless fermions (for simplicity) with only nearest-neighbor (NN) hopping reads as

$$H = -\sum_{\langle i,j \rangle} (t_{ij} a_i^\dagger b_j + H.c), \tag{8}$$

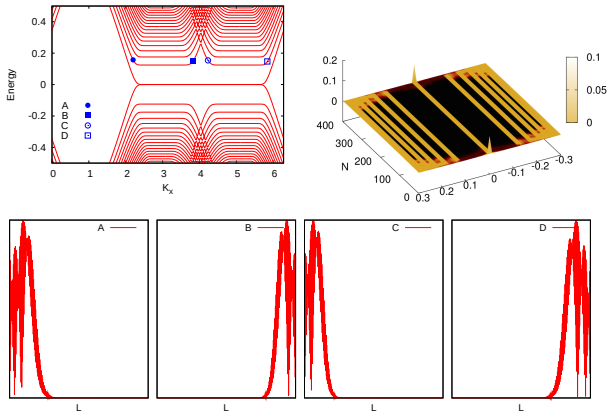

FIG. 7: (Color online) The energy spectrum, LDOS and wave-function in a real magnetic field. In this case, the Landau levels are clearly developed. The Fermi energy crosses the first Landau level at four points A, B, C, and D, in which A, B and C, D belong to two different valleys.

where a_i and b_j are the fermionic annihilation operators on sites of two inter-penetrating triangular sub-lattices. $\langle i, j \rangle$ stands for the summation over three NN sites. In pristine graphene, the hopping amplitudes along three directions are equal. The above Hamiltonian can be represented by a set of Harpers equation, due to the translational symmetry along the x-direction. One can then easily obtain the energy momentum relation numerically. The energy spectrum and the local density of states (LDOS) for isotropic zigzag edge is shown in Fig. 6. The Dirac points are located at $k_x = 2\pi/3$ and $k_x = 4\pi/3$. In the vicinity of the Dirac points the dispersion is linear. The edge states at $E = 0$ arise due to charge accumulation on two different sub-lattices, causing peaks in LDOS, which possibly can be detected in STM measurement.

The orbital effect of the real magnetic field can be captured by introducing Peierls phase in the NN hopping amplitudes, $t_{ij} \to t_{ij} e^{2\pi i \phi_{ij}}$. ϕ_{ij} is related to the magnetic vector potential as

$$\phi_{ij} = \frac{e}{hc} \int_i^j \vec{A} \cdot d\vec{l}. \tag{9}$$

In the presence of magnetic field, the linear dispersions around the Dirac points quenche into sets of Landau levels at well separated energies, as shown in Fig. 7. It is evident from this figure that the wave functions living on the same edge share identical chirality. For example, wave-functions on left side of each valleys, A and C, are located on left zigzag edge, whereas those on the right side of each valleys, B and D, are located on right zigzag edge.

One can introduce the axial magnetic field (b) by locally modifying the hopping amplitudes. One particular way of such deformation is the following. We here modify the hopping only along one of the three bonds, oriented orthogonal to the zigzag edge. It smoothly varies from

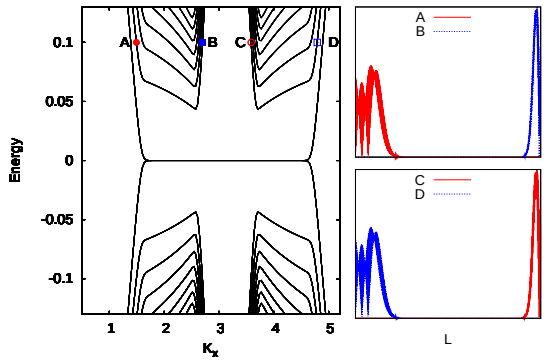

FIG. 8: (Color online) The energy spectrum (left) and the wave functions (right) in a strain field. The hopping, perpendicular to zigzag edge, ranges from t - W/2 to t + W/2 with W = 1.0 from one edge to the other. Here we set $t = 1$. Wave-functions localized on one edge, live on opposite side at two valley, explicitly, A(B) and D (C) are localized on left (right) edge. Henceforth, the edge states near two valleys have different chirality. In the presence of real magnetic fields, situation is reversed, i.e., wave-functions on left (A,C) (right (B,D)) side of each valleys are located on left (right) edge.

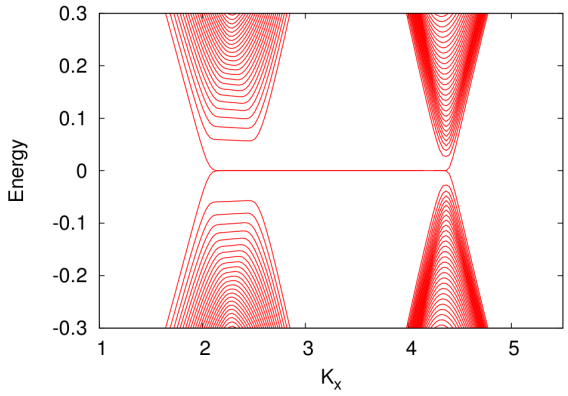

FIG. 9: (Color online) The energy spectrum when B ≈ b. The Landau levels are only developed in one valley and the Dirac cone is recovered at the other one.

$t - \frac{W}{2}$ to $t + \frac{W}{2}$, where $W \leq t$, from one edge of the system to the other, separated by 300 unit cells. With such simple deformation, one ends up with slightly inhomogeneous Fermi velocities and thus LL energies. Nevertheless, we can immediately see from Fig. 8 that chirality of the edge modes are opposite at each edge in the presence of axial/pseudo magnetic field [4], as we discussed in the manuscript.

Upon tuning the relative strength of the fields, one can achieve an interesting limit, $b \approx B$. Only one of the Dirac points is then exposed to finite magnetic field, $2B$ or $2b$. Therefore, the energy spectrum near that Dirac point is composed of Landau levels. On the other hand, the system remains semi-metallic in the vicinity of the other Dirac point [5]. This scenario is depicted in Fig. 9.

III. DIRAC LANDAU LEVELS WITH SYMMETRY BREAKING TERMS

Let us now compute the LL spectrum of the emergent single particle Hamiltonian, containing various symmetry breaking terms. For our purpose, we keep both the antiferromagnet ($\vec{N}$) and the quantum spin Hall ($\vec{C}$) orders besides the free Dirac Hamiltonian with real and axial vector potentials. The resulting Hamiltonian reads as

$$\begin{aligned} H_{HF} &= I_2 \otimes i\gamma_0\gamma_i \left(\hat{q}_i - A_i - i\gamma_3\gamma_5 a_i\right) - \left(\vec{N}\cdot\vec{\sigma}\right)\otimes\gamma_0 \\ &- \left(\vec{C}\cdot\vec{\sigma}\right)\otimes i\gamma_1\gamma_2 + \lambda_z\left(\sigma_3\otimes I_4\right), \end{aligned} \tag{10}$$

if one wishes to keep the Zeeman coupling (λ_z) as well. However, in comparison to the broken symmetry order parameters, the Zeeman term is much smaller and one can neglect it. Then all spin projections are equivalent and we choose $\vec{N} = (N, 0, 0)$ and $\vec{C} = (C, 0, 0)$ for the ease of calculation. Even in the presence of symmetry breaking terms two inequivalent valleys are decoupled and one can cast H_{HF} is block diagonal form $H_+ \oplus H_-$, where

$$\begin{aligned} H_\pm &= \pm I_2\otimes\sigma_1(\hat{q}_1 \mp a_1 - A_1) + I_2\otimes\sigma_2(\hat{q}_2 \mp a_2 - A_2) \\ &- (\sigma_3\otimes\sigma_3)\,N \mp (\sigma_3\otimes\sigma_3)\,C, \end{aligned} \tag{11}$$

after exchanging the second and third 2×2 blocks. Using the unitary rotations U_1 and U_2, defined in sec. I, one can cast $H_\pm$ as

$$H_\pm \to i\gamma_0\gamma_i\left(\hat{q}_i \mp a_i - A_i\right) - \gamma_0\left(N \pm C\right). \tag{12}$$

Therefore the spectrum of H_{HF} is composed of two sets of inequivalent LLs, at energies $\pm\sqrt{2n(b\pm B) + (N\pm C)^2}$, for $n \geq 1$ and $\pm|N \pm C|$ when $n = 0$.

IV. GAP EQUATIONS

The ground state energy per unit area at half-filling in the presence of two symmetry breaking order parameters reads as

$$E[N, C] = \frac{N^2}{4g_a} + \frac{C^2}{4g_c} + E_0[N, C], \tag{13}$$

as shown in the main text. $E_0[N, C]$ is the ground state energy of the effective single particle Hamiltonian H_{HF}. At Half-filling, the ground state of H_{HF} has all the states at negative energies filled, while those at positive energies at completely empty, yielding

$$\begin{aligned} E_0[N, C] &= \frac{1}{4\pi}\sum_{n\geq 1}\left((b+B)e_{n,+} + (b-B)e_{n,-}\right) \\ &+ \frac{1}{4\pi}\left((b+B)(N+C) + (b-B)|N-C|\right), \end{aligned} \tag{14}$$

where $e_{n,\sigma} = \sqrt{2n(b+\sigma B) + (N+\sigma C)^2}$, for $\sigma = \pm 1$. In the main text of the paper, we argued that unless $g_a \equiv g_c$, the anti-ferromagnet and the spin Hall order cannot coexist. For $g_a > g_c$, i.e when the on-site repulsion (U) is stronger than the next neighbor one (V_2), at half-filling the ground state configuration is with $N \neq 0$, while $C \equiv 0$. Minimizing the ground state energy, $E[N,0]$, with respect to N, then yields the gap equation at half filling

$$\frac{1}{4g} = \frac{1}{4\pi^{3/2}} \int_0^\infty \frac{ds}{s^{3/2}}\, e^{-sm^2} \sum_{\sigma=\pm 1} (b+\sigma B)\, \frac{2s}{e^{2s(b+\sigma B)}-1} + \frac{b}{2\pi m}, \tag{15}$$

where $g \equiv g_a$. The first term on the R. H. S. counts the contribution of all the filled LLs with $n \geq 1$, and it is ultra-violet divergent, while the second term on the R. H. S. arises only from the ZLL. However, the divergence can be regulated by defining the zero field critical interaction for ordering as

$$\frac{1}{g_*} = \frac{2\Lambda}{\sqrt{\pi}} \int_0^\infty \frac{ds}{s^{3/2}}, \tag{16}$$

after $\pi/g \to 1/g$, so that the physical gap remains cut-off (Λ) independent. The cut-off (Λ) defines the range of energy, over which the dispersion is approximately linear. Defining the strength of the interaction as

$$\delta = \frac{1}{\Lambda g} - \frac{1}{\Lambda g_*}, \tag{17}$$

where δ measures the deviation of the interaction from the zero field critical interaction for insulation, one can cast the gap equation as

$$x\left(1+\frac{1}{q}\right) = \frac{\delta}{m} + \frac{1}{\sqrt{\pi}}\left(1+\frac{1}{\sqrt{q}}\right) f(x). \tag{18}$$

Here we introduced new variables, $x = \frac{b+B}{m^2}$, and $q = \frac{b+B}{b-B}$ and the function $f(x)$ reads as

$$f(x) = \frac{m\sqrt{x}}{\sqrt{\pi}}\left(1+\frac{1}{\sqrt{q}}\right) \int_0^\infty \frac{ds}{s^{3/2}} \left[\frac{2se^{-s/x}}{e^{2s}-1} - 1\right]. \tag{19}$$

Similarly, one can arrive at the gap equation for the $\sigma_{xy} = \pm e^2/h$ Hall state, which on the other hand reads as

$$\frac{1}{4g} = \frac{1}{4\pi^{3/2}} \int_0^\infty \frac{ds}{s^{3/2}}\, e^{-sm^2} \sum_{\sigma=\pm 1} (b+\sigma B)\, \frac{2s}{e^{2s(b+\sigma B)}-1} + \frac{b+B}{4m\pi}, \tag{20}$$

where $g \equiv g_c$, assuming $N > C$ or $g_a > g_c$. Here the contribution from the filled LLs (first term on R. H.S.) is identical to that in Eq. (15), but the ZLL contribution is different from that in Eq. (15), since only fewer states contributes to the ground state energy when the chemical potential is tuned close to the spin polarized gap (N). After performing similar exercise, one can finds the gap equation to be

$$x = \frac{\delta}{m} + \frac{1}{\sqrt{\pi}}\left(1+\frac{1}{\sqrt{q}}\right) f(x). \tag{21}$$

For $\delta = 0$ ($g = g_*$) and $b = 300$ T, solutions of the gap equations are at $x = x_0 = 5.0537$ and 17.9226 for $B = 0$ T, respectively. For $B = 50$ T, the solutions are at $x_0 = 5.741$ and 15.378.[6] For a finite $\delta > 0$ ($g < g_*$), the solutions can only be found at $x > x_0$. Hence, for realistic strength of two fields, one can safely expand $f(x)$ for large argument of x, leaving us with simple *algebraic* equations for the interaction induced activation gap for $\sigma_{xy} = 0, \pm e^2/h$ Hall state, read as

$$x\left(1+\frac{1}{q}\right) - \frac{\delta}{m} - \left(1+\frac{1}{\sqrt{q}}\right)\left(\sqrt{x}u + \frac{v}{\sqrt{x}} + \mathcal{O}(x^{-3/2})\right) = 0, \tag{22}$$

$$x - \frac{\delta}{m} - \left(1+\frac{1}{\sqrt{q}}\right)\left(\sqrt{x}u + \frac{v}{\sqrt{x}} + \mathcal{O}(x^{-3/2})\right) = 0, \tag{23}$$

respectively. The coefficients are $u = 2.0652$ and $v = 0.924$. The numerical solutions of the gaps are shown in the main part of the paper, for a set of realistic strengths of interactions ($\delta > 0$) in graphene.

[1] I. F. Herbut, Phys. Rev. B **78**, 205433 (2008); B. Roy, *ibid* **84**, 035458 (2011); *ibid* **85**, 165453 (2012).

[2] I. F. Herbut, Phys. Rev. B, **76**, 085432 (2007).

[3] V. P. Gusynin, et. al., Phys. Rev. Lett. **95**, 146801 (2005); N. M. R. Peres, et. al., Phys. Rev. B **72**, 174406 (2005); I. F. Herbut, *ibid* **75**, 164411 (2007).

[4] Y. Chang, T. Albash, and S. Hass, Phys. Rev. B **86**, 125402 (2012).

[5] T. Low and F. Guinea, Nano Lett. **10**, 3551 (2010).

[6] I. F. Herbut, B. Roy, Phys. Rev. B **77**, 245438 (2008); B. Roy, I. F. Herbut, *ibid*, **83**, 195422 (2011).

[7] Similar scaling function with only real magnetic field ($B \neq 0$ but $b = 0$) can also be found using 'functional renormalization group' approach. See, D. D. Scherer, and H. Gies, Phys. Rev. B **85**, 195417 (2012).